

Anomalous Damping of a Low Frequency Vibrating Wire in Superfluid $^3\text{He-B}$ due to Vortex Shielding

D.I. Bradley · M.J. Fear · S.N. Fisher ·
A.M. Guénault · R.P. Haley · C.R. Lawson ·
G.R. Pickett · R. Schanen · V. Tsepelin

Received: 25 July 2013 / Accepted: 19 September 2013 / Published online: 2 October 2013
© The Author(s) 2013. This article is published with open access at Springerlink.com

Abstract We have investigated the behaviour of a large vibrating wire resonator in the B-phase of superfluid ^3He at zero pressure and at temperatures below 200 μK . The vibrating wire has a low resonant frequency of around 60 Hz. At low velocities the motion of the wire is impeded by its intrinsic (vacuum) damping and by the scattering of thermal quasiparticle excitations. At higher velocities we would normally expect the motion to be further damped by the creation of quasiparticles from pair-breaking. However, for a range of temperatures, as we increase the driving force we observe a sudden decrease in the damping of the wire. This results from a reduction in the thermal damping arising from the presence of quantum vortex lines generated by the wire. These vortex lines Andreev-reflect low energy excitations and thus partially shield the wire from incident thermal quasiparticles.

Keywords Vibrating Wire · Superfluid Helium · Turbulence · Vortex Shielding

1 Introduction

Oscillating probes have been used extensively in quantum fluids research. In recent years there have been many investigations of quantum turbulence in superfluid ^4He using quartz tuning forks [1, 2], oscillating microspheres [3] and vibrating wire resonators [4, 5]. Vibrating wire resonators are particularly useful for studying quasiparticle excitations [6, 7] and quantum turbulence [8–12] in superfluid ^3He .

One of the simplest methods of creating turbulence in the superfluid is to move an object through it at a sufficiently high velocity. At low velocity and at zero temperature, motion through the superfluid occurs without dissipation. However above

D.I. Bradley · M.J. Fear · S.N. Fisher · A.M. Guénault · R.P. Haley · C.R. Lawson (✉) ·
G.R. Pickett · R. Schanen · V. Tsepelin
Department of Physics, Lancaster University, Lancaster, United Kingdom
e-mail: c.lawson@lancaster.ac.uk

some critical velocity v_c dissipation may occur by breaking the superfluid to form excitations. For a vibrating wire in superfluid $^3\text{He-B}$, the critical velocity is given by [13–15] $v_c = v_L/3$ where $v_L = \Delta/p_F$ is the Landau critical velocity. Previous experiments [16, 17] have shown that vortex lines are also generated above this critical velocity.

At finite temperatures, the motion of an object in superfluid ^3He is damped by thermal quasiparticle excitations [18–20]. The mean free path of thermal quasiparticles vastly exceeds the dimensions of the experimental cell at temperatures below $T = 200 \mu\text{K}$. In this ballistic regime, the thermal damping on a vibrating wire is proportional to the flux of incident quasiparticles, which falls exponentially with the Boltzmann factor $\exp(-\Delta/kT)$ where Δ is the superfluid energy gap.

Quantum vortex lines are particularly easy to detect in superfluid $^3\text{He-B}$ at low temperatures since they have a large cross-section for the Andreev reflection of quasiparticles [16, 21–23]. Consequently a vibrating wire surrounded by vortices is partially screened from incoming thermal quasiparticles leading to a *drop* in the observed damping. In previous measurements this effect was only observed when the vortices were generated from a remote source. This is because vortices are usually only generated above the critical velocity where the damping is heavily dominated by pair-breaking.

Here we present measurements carried out using a large vibrating wire designed to have a very low resonant frequency. We refer to this device as a ‘floppy wire’. Below we present measurements which show a pronounced drop in the damping on the wire at velocities just below the pair-breaking critical velocity. This indicates that there are substantial amounts of vortices generated close to the critical velocity where the damping due to pair-breaking is small.

2 Experimental Details

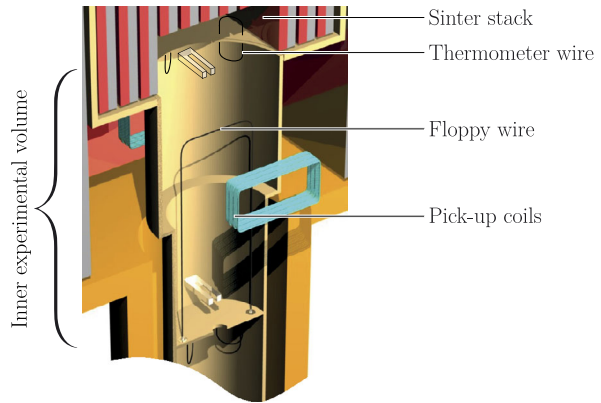
The floppy wire is shown in Fig. 1. The device was designed to allow measurements at arbitrary frequencies by using a high frequency probe current and pick-up coils to measure the wire position [24]. A similar device was recently used to probe the frequency dependence of grid turbulence [25] in superfluid ^4He . Here we describe measurements using conventional vibrating wire techniques [18, 26, 27] at the resonant frequency of the wire.

The floppy wire is made from an insulated copper clad single filament NbTi wire with a diameter of 0.1 mm. This is bent around a former into a goalpost shape of height 25 mm with a crossbar length of $D = 9$ mm. The device is installed in the inner section of a ‘Lancaster-style’ nuclear demagnetization cell [28] as shown in Fig. 1. The measurements below were taken in $^3\text{He-B}$ at zero pressure in a vertical magnetic field of $B = 61$ mT provided by a large demagnetization magnet in the 4.2 K helium bath.

When driven by an ac current $I_0 e^{i\omega t}$ the crossbar of the floppy wire experiences a Lorentz force of amplitude

$$F_0 = BDI_0. \quad (1)$$

Fig. 1 Part of the inner experimental volume of a “Lancaster style” nuclear demagnetization cell showing the floppy wire device. Also shown are pick-up coils which may be used in future experiments to allow measurements at arbitrary frequencies (Color figure online)



At the resonant frequency, the amplitude of the driving force is equal to the amplitude of the damping force opposing the motion. As the wire moves through the vertical magnetic field a Faraday voltage

$$V = BDv \quad (2)$$

is induced, where v is the velocity of the wire crossbar.

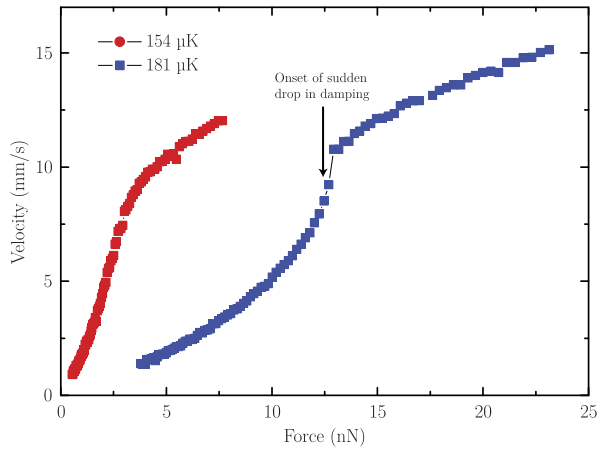
The induced voltage amplitude V_0 is measured using a lock-in amplifier, referenced to the function generator which provides the driving current. In vacuum at 4.2 K the wire had a resonant frequency of $f_0 = 66.394$ Hz and a frequency width, corresponding to the intrinsic damping, of $\Delta f_2 = 0.012$ Hz.

The measurements below were made by slowly increasing the driving force whilst measuring the resonant signal voltage. This allows us to infer the damping force and velocity of the wire using equations (1) and (2), respectively. The frequency of the wire is adjusted for each measurement to maintain the resonance condition. This is done by minimising the component of the signal which is out-of-phase with the driving current (at resonance the velocity response should be entirely in-phase with the driving force). The drive sweeps were repeated as the experiment warmed over a temperature range of around 150 μK to 200 μK . The temperature (thermal quasiparticle density) was independently measured [31] at each measurement point using a neighbouring NbTi thermometer wire of diameter ≈ 4.5 μm . The dissipation from the floppy wire is quite significant so the cell temperature rises a little when the wire is driven at the highest velocities.

3 Results

Figure 2 show the results of drive sweeps at two different temperatures. Here we plot the amplitude of the wire velocity versus the amplitude of the damping force. At the lowest temperature, the wire velocity is roughly proportional to the damping force below a velocity $v \approx 9$ mm s^{-1} . At higher velocities the damping force increases dramatically as energy is dissipated by breaking Cooper pairs and generating quasiparticles. Similar behaviour is observed for conventional vibrating wire resonators

Fig. 2 The amplitude of the wire velocity versus the amplitude of the damping force for drive sweeps measured at two different temperatures. The onset of anomalous damping is indicated (Color figure online)



[18] and for tuning forks [29]. At higher temperatures the response at low velocities is non-linear due to the thermal damping force, see below. Furthermore the velocity shows a sudden jump upwards indicating a drop in the damping.

In the low temperature ballistic regime the total damping force F_{Tot} exerted on a mechanical resonator may be broken down into three separate parts [18]

$$F_{Tot} = F_i + F_{PB} + F_{th}. \tag{3}$$

Here F_i represents the intrinsic damping from internal losses in the wire. This is approximately proportional to the velocity and is independent of temperature. The force due to generating quasiparticles by breaking Cooper pairs is given by F_{PB} . This force rises steeply above the critical velocity [13–15], $v_c = v_L/3 \approx 9 \text{ mm s}^{-1}$. The thermal damping force arises from scattering with thermal quasiparticle excitations, but is enhanced enormously by Andreev scattering from the superfluid back-flow around the wire [18–20]. The thermal damping force can be written as

$$F_{Th} = b \left(1 - e^{-\frac{\lambda P_F v}{k_B T}} \right) \tag{4}$$

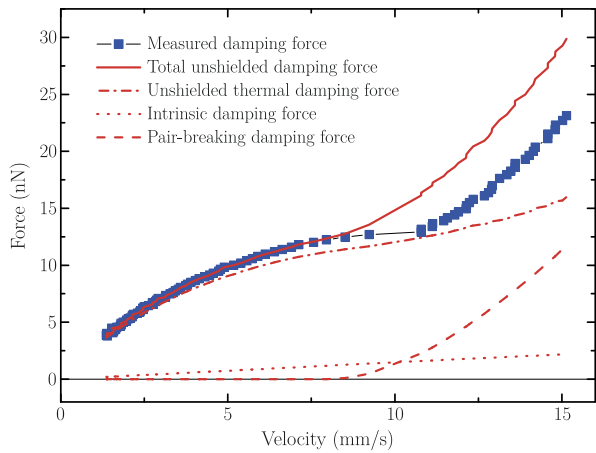
where b is a constant proportional to the wire diameter and λ is a dimensionless factor of order unity which depends on the wire geometry and the superfluid backflow. This form of the thermal damping has been found to give excellent agreement with previous vibrating wire [18] and tuning fork [29] measurements.

In principle Eq. (3) should include a force due to the generation of vortices. However, in practice this force is usually insignificant. This ‘vortex shedding’ force has only been observed as a very small anomaly, at velocities a little below the pair-breaking critical velocity, associated with localised vortex production by remnant vortices pinned to surface imperfections [32, 33].

However the above considerations cannot account for the sudden upwards jump in velocity shown for the higher temperature data in Fig. 2. This behavior indicates the presence of vortices which partially screen the wire from thermal quasiparticles. To model this behaviour we re-write the damping force on the wire as

$$F_{Tot} = F_i + F_{PB} + (1 - f)F_{Th} \tag{5}$$

Fig. 3 The damping force acting on the floppy wire as a function of velocity. The measured damping force is shown by the square points. The dotted, dashed and dash-dotted lines show the contributions of the intrinsic, pair-breaking and unshielded thermal damping forces, respectively. The solid line gives the expected total force in the absence of shielding (Color figure online)



where f measures the fraction of thermal quasiparticles incident on the wire which are Andreev reflected by vortices generated by the wire. For a given configuration of vortices, the fractional screening f should be inversely proportional to the temperature [16].

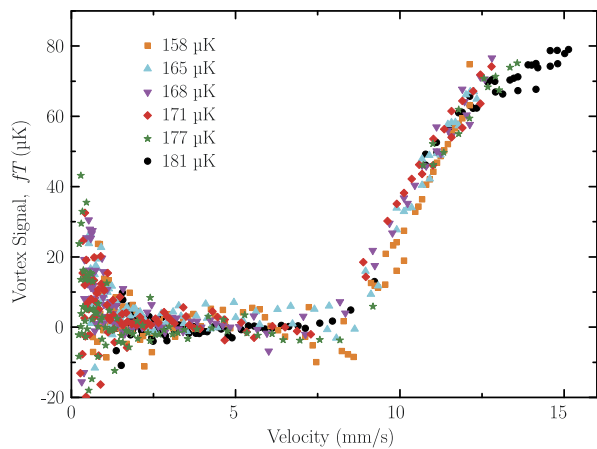
We cannot directly measure the separate contributions to the damping given in Eq. (5). However, by comparing the low velocity damping of the floppy wire with that of the thermometer wire, we can infer the intrinsic damping of the floppy wire F_i as well as the unshielded thermal damping force F_{Th} at low velocities. To infer the thermal force at higher velocities, we need to find the value of λ in Eq. (4). We do this by fitting the measurements at moderate velocities, where there is no shielding from vortices. To find the pair-breaking contribution F_{PB} we first use a trial function for the fractional shielding f which is inversely proportional to temperature. We can then subtract the intrinsic and shielded thermal forces to leave the pair-breaking force. The pair-breaking force should be independent of temperature, so if our trial function for f is correct then the curves for the pair-breaking force at different temperatures will collapse onto a single line. If not, we adjust our trial function until the curves do collapse. We can then fit the pair-breaking force to a smooth function of velocity. Once we have this, we can reanalyse the data to extract the fractional shielding f for all of the drive sweep measurements.

The various contributions to the total damping are shown in Fig. 3 for the drive sweep taken at a temperature of $T = 181 \mu\text{K}$. The points show the measured values. The dotted and dashed lines show the inferred contributions from the intrinsic force F_i and the pair-breaking force F_{PB} , respectively. The dash-dotted line shows the unshielded thermal damping contribution F_{Th} . The solid line shows the sum of these three forces, corresponding to the total expected force in the absence of shielding, Eq. (3).

To obtain the fractional shielding from vortices, f , we take the difference between the expected unshielded force and the measured force and divide this by the unshielded thermal force, F_{Th} .

The results are shown in Fig. 4. Here we plot the fractional shielding f multiplied by temperature T versus the wire velocity for various different temperatures.

Fig. 4 The vortex signal, fT , as a function of velocity for a range of temperatures, see text (Color figure online)



The product fT defines the ‘vortex signal’ which gives a measure of the amount of vortices generated which ‘self-shield’ the wire from scattering with thermal excitations. The data at different temperatures collapse quite well onto a single curve which justifies assumptions made in the analysis.

It is interesting to note that the fractional screening f approaches 50 % at the highest velocities and the lowest temperatures. This is roughly twice larger than typical screening values observed using vibrating wire detectors [16, 17]. Such a large screening suggests that there is a very dense tangle of vortices in the immediate vicinity of the wire. However, it is not possible to infer the vortex line density without knowing the spatial distribution of the vortices. This could be found in future experiments using vibrating wire detectors [9].

4 Conclusions

We have made the first measurements of ‘self-shielding’ of a wire resonator by vortices. The wire generates vortices that shield the wire from thermal quasiparticles. Unlike previous vibrating wire resonators, a substantial amount of vorticity is generated at, or slightly below, the onset velocity for pair-breaking. This allows the effects of the shielding to be observable even in the presence of a substantial damping force from pair-breaking. It is interesting to note that pair-breaking below the Landau velocity is only possible by the temporary population of bound-states at the wire surface [14, 30], and that this same mechanism could be responsible for the hydrodynamic instability which leads to the generation of vortices [30]. Vortex production and pair-breaking may thus be closely linked. Indeed, we find that they have very similar onset velocities. The relative amounts of pair-breaking and vortex production may be dependent on the frequency of oscillation. We plan to study this in the future by using ‘floppy wire’ techniques [24, 25] to allow measurements at different frequencies.

Acknowledgements We thank S.M. Holt, A. Stokes and M.G. Ward for excellent technical support. This research is supported by the UK EPSRC and by the European FP7 Programme MICROKELVIN Project, no. 228464.

Open Access This article is distributed under the terms of the Creative Commons Attribution License which permits any use, distribution, and reproduction in any medium, provided the original author(s) and the source are credited.

References

1. R. Blaauwgeers, M. Blazkova, M. Človečko, V. Eltsov, R. de Graaf, J. Hosio, M. Krusius, D. Schmoranzler, W. Schoepe, L. Skrbek, P. Skyba, R. Solntsev, D. Zmeev, J. Low Temp. Phys. **146**, 537 (2007)
2. D.I. Bradley, M. Človečko, M.J. Fear, S.N. Fisher, A.M. Guénault, R.P. Haley, C.R. Lawson, G.R. Pickett, R. Schanen, V. Tsepelin, P. Williams, J. Low Temp. Phys. **165**(3–4), 114 (2011)
3. J. Jäger, B. Schuderer, W. Schoepe, Phys. Rev. Lett. **74**, 566 (1995)
4. D.I. Bradley, D.O. Clubb, S.N. Fisher, A.M. Guénault, R.P. Haley, C.J. Matthews, G.R. Pickett, K.L. Zaki, J. Low Temp. Phys. **138**(3/4), 493 (2005)
5. R. Goto, S. Fujiyama, H. Yano, Y. Nago, N. Hashimoto, K. Obara, O. Ishikawa, M. Tsubota, T. Hata, Phys. Rev. Lett. **100**, 045301 (2008)
6. M. Bartkowiak, S. Daley, S. Fisher, A. Guénault, G. Plenderleith, R. Haley, G. Pickett, P. Skyba, Phys. Rev. Lett. **83**, 3462 (1999)
7. S. Fisher, A. Guénault, N. Mulders, G. Pickett, Phys. Rev. Lett. **91**, 105303 (2003)
8. D.I. Bradley, D.O. Clubb, S.N. Fisher, A.M. Guénault, R.P. Haley, C.J. Matthews, G.R. Pickett, V. Tsepelin, K. Zaki, Phys. Rev. Lett. **95**, 035302 (2005)
9. D.I. Bradley, D.O. Clubb, S.N. Fisher, A.M. Guénault, R.P. Haley, C.J. Matthews, G.R. Pickett, V. Tsepelin, K. Zaki, Phys. Rev. Lett. **96**(3), 035301 (2006)
10. D.I. Bradley, S.N. Fisher, A.M. Guénault, R.P. Haley, S. O’Sullivan, G.R. Pickett, V. Tsepelin, Phys. Rev. Lett. **101**, 065302 (2008)
11. Y. Nago, M. Inui, R. Kado, K. Obara, H. Yano, O. Ishikawa, T. Hata, Phys. Rev. B **82**, 224511 (2010)
12. D.I. Bradley, S.N. Fisher, A.M. Guénault, R.P. Haley, G.R. Pickett, D. Potts, V. Tsepelin, Nat. Phys. **7**, 473 (2011)
13. S.N. Fisher, A.M. Guénault, C.J. Kennedy, G.R. Pickett, Phys. Rev. Lett. **67**, 1270 (1991)
14. C.J. Lambert, Physica B **178**, 294 (1992)
15. S.N. Fisher, A.M. Guénault, C.J. Kennedy, G.R. Pickett, Phys. Rev. Lett. **69**, 1073 (1992)
16. D.I. Bradley, S.N. Fisher, A.M. Guénault, M.R. Lowe, G.R. Pickett, A. Rahm, R.C.V. Whitehead, Phys. Rev. Lett. **93**(23), 235302 (2004)
17. S.N. Fisher, A.J. Hale, A.M. Guénault, G.R. Pickett, Phys. Rev. Lett. **86**(2), 244 (2001)
18. S.N. Fisher, A.M. Guénault, C.J. Kennedy, G.R. Pickett, Phys. Rev. Lett. **63**, 2566 (1989)
19. M.P. Enrico, S.N. Fisher, R.J. Watts-Tobin, J. Low Temp. Phys. **98**, 81 (1995)
20. S.N. Fisher, G.R. Pickett, R.J. Watts-Tobin, J. Low Temp. Phys. **83**, 225 (1991)
21. C. Barenghi, Y. Sergeev, N. Suramlishvili, Phys. Rev. B **77**, 104512 (2008)
22. Y.A. Sergeev, C.F. Barenghi, N. Suramlishvili, P.J. van Dijk, Europhys. Lett. **90**(5), 56003 (2010)
23. S. Fujiyama, A. Mitani, M. Tsubota, D.I. Bradley, S.N. Fisher, A.M. Guénault, R.P. Haley, G.R. Pickett, V. Tsepelin, Phys. Rev. B **81**(18), 180512 (2010)
24. D. Bradley, M. Človečko, M. Fear, S. Fisher, A. Guénault, R. Haley, C. Lawson, G. Pickett, R. Schanen, V. Tsepelin, P. Williams, J. Low Temp. Phys. **165**(3–4), 114 (2011)
25. D.I. Bradley, S.N. Fisher, A.M. Guénault, R.P. Haley, M. Kumar, C.R. Lawson, R. Schanen, P.V.E. McClintock, L. Munday, G.R. Pickett, M. Poole, V. Tsepelin, P. Williams, Phys. Rev. B **85**, 224533 (2012)
26. R. Donnelly, A.H. Hallett, Ann. Phys. **3**(3), 320 (1958)
27. D. Carless, H. Hall, J. Hook, J. Low Temp. Phys. **50**(5–6), 583 (1983)
28. G. Pickett, S. Fisher, Physica B, Condens. Matter **329–333**(1), 75 (2003). Proceedings of the 23rd International Conference on Low Temperature Physics
29. D.I. Bradley, P. Crookston, S.N. Fisher, A. Ganshin, A.M. Guénault, R.P. Haley, M.J. Jackson, G.R. Pickett, R. Schanen, V. Tsepelin, J. Low Temp. Phys. **157**(5–6), 476 (2009)
30. A. Calogeracos, G.E. Volovik, J. Exp. Theor. Phys. **88**, 40 (1999)
31. C. Bäuerle, Y.M. Bunkov, S.N. Fisher, H. Godfrin, Phys. Rev. B **57**, 14381 (1998)
32. D.I. Bradley, Phys. Rev. Lett. **84**, 1252 (2000)
33. D. Bradley, S. Fisher, A. Ganshin, A. Gunault, R. Haley, M. Jackson, G. Pickett, V. Tsepelin, J. Low Temp. Phys. **171**(5–6), 582 (2013)